bioRxiv preprint doi: https://doi.org/10.1101/2024.03.06.583765; this version posted March 12, 2024. The copyright holder for this preprint (which was not certified by peer review) is the author/funder. All rights reserved. No reuse allowed without permission.

Title: The wake and sleep-modulating neurons of the lateral hypothalamic area demonstrate a differential pattern of degeneration in Alzheimer's disease.

bioRxiv preprint doi: https://doi.org/10.1101/2024.03.06.583765; this version posted March 12, 2024. The copyright holder for this preprint (which was not certified by peer review) is the author/funder. All rights reserved. No reuse allowed without permission.

Title: The wake and sleep-modulating neurons of the lateral hypothalamic area demonstrate a differential pattern of degeneration in Alzheimer's disease.

Abhijit Satpati[1], Alexander V. Soloviev[1], Felipe L. Pereira[1], Mihovil Mladinov[1], Eva Larsen[1], Renata E. P. Leite[2,3], Claudia K. Suemoto[2,4], Roberta D. Rodriguez[5], Vitor R. Paes[2], Christine Walsh[1], Salvatore Spina[1], William W. Seeley[1], Carlos A. Pasqualucci[5], Wilson Jacob Filho[5], Thomas C. Neylan[1,6] and Lea T. Grinberg[1,2,3*]

1. Memory and Aging Center, University of California San Francisco, USA.
2. Physiopathology in Aging Laboratory (LIM-22), Department of Internal Medicine, University of Sao Paulo Medical School, Sao Paulo, Brazil.
3. Department of Pathology, University of Sao Paulo Medical School, Sao Paulo, Brazil.
4. Division of Geriatrics, Department of Internal Medicine, University of Sao Paulo Medical School, Sao Paulo, Brazil
5. University of Sao Paulo Medical School, Sao Paulo, Brazil
6. Department of Psychiatry, University of California San Francisco, San Francisco, California, USA

*Corresponding author

bioRxiv preprint doi: https://doi.org/10.1101/2024.03.06.583765; this version posted March 12, 2024. The copyright holder for this preprint (which was not certified by peer review) is the author/funder. All rights reserved. No reuse allowed without permission.

Abstract

Background: Sleep-wake dysfunction is an early and common event in Alzheimer's disease (AD). The lateral hypothalamic area (LHA) regulates the sleep and wake cycle through wake-promoting orexinergic and sleep-promoting melanin-concentrating hormone (MCH) neurons. These neurons share close anatomical proximity with functional reciprocity. This study investigated the pattern of neuronal loss (ORX and MCH) in the LHA in AD. Understanding the degeneration pattern of these neurons will be instrumental in designing potential therapeutics to slow down the disease progression and remediate the sleep-wake dysfunction in AD.

Methods: Postmortem human brain tissue of subjects with AD (across progressive stages) and controls were examined using unbiased stereology. Neuronal counting was done using double immunohistochemistry with ORX, pTau (CP13), and MCH, pTau (CP13) labeled neurons on formalin-fixed, celloidin-embedded tissue.

Results: We observed a progressive decline in orexinergic (ORX) neurons and a relative preservation of the melanin-concentrating hormone (MCH) neurons. The decline in ORX neurons was seen from BB 2 (56%, $p=0.0634$). By the late stage of the disease (BB 5-6), the decline in ORX neurons was 76% ($p=0.0043$). In contrast, the MCH neurons demonstrated an insignificant decline by BB 6 (25%, $p=0.1313$).

Conclusions: Our data demonstrated very early substantial ORX neuronal loss in the LHA, while MCH neurons were resilient to AD pTau accumulation. Interventions capable of preventing ORX neuronal loss and inhibiting pTau accumulation in the LHA can reinstate sleep-wake dysfunction in AD and possibly prevent the progression of the disease.

Keywords: Lateral hypothalamic area, Melanin-concentrating hormone, Orexin, Subcortical neuromodulatory, Sleep-wake neurons, Unbiased stereology.

bioRxiv preprint doi: https://doi.org/10.1101/2024.03.06.583765; this version posted March 12, 2024. The copyright holder for this preprint (which was not certified by peer review) is the author/funder. All rights reserved. No reuse allowed without permission.

Introduction:

Alzheimer's disease (AD) is the most common form of dementia, and approximately 6.7 million Americans 65 years or older have the disease[1]. AD is an age-dependent, devastating, progressive neurodegenerative disorder that typically progresses from a preclinical phase (without any cognitive symptoms) through mild cognitive impairment to severe dementia[2]. This preclinical phase of the disease is associated with the accumulation of AD pathology[2]. Sleep-wake dysfunction is often seen in the preclinical phase of the disease preceding the onset of cognitive symptoms[3]. Excessive daytime sleepiness, shorter N3 stage of non-REM sleep, and sundowning characterize AD patients' clinical sleep profile[4,5]. Previous studies from our group have demonstrated that sleep-wake dysfunction or changes in the sleep phenotypes in AD were correlated with a significant loss of subcortical wake-promoting neurons[6,7].

The subcortical lateral hypothalamic area (LHA), with two of its neuropeptides, orexin or hypocretin (ORX) and melanin-concentrating hormone (MCH), plays a critical role in maintaining sleep-wake homeostasis. The ORX regulates arousal and wakefulness through modulation of the locus coeruleus[8]. Various studies on experimental animals have shown that the neuropeptide ORX is involved in locomotor activity, attention, cognition, feeding behavior reward, and thermogenesis by regulating prolactin, growth hormones, acetylcholine, and corticosterone levels[8–12]. Liguori et al. demonstrated an increase in CSF ORX levels in patients with moderate to severe AD was associated with sleep dysfunction and decline in cognition[13]. Using an *in vitro* model and AD patient samples, Davies et al. demonstrated that ORX mediates induction of ERK1/2 phosphorylation and provides neuroprotection[14]. In addition to AD, loss of

bioRxiv preprint doi: https://doi.org/10.1101/2024.03.06.583765; this version posted March 12, 2024. The copyright holder for this preprint (which was not certified by peer review) is the author/funder. All rights reserved. No reuse allowed without permission.

ORX neurons was also reported in Parkinson's disease, Huntington's disease, and Multiple sclerosis[15].

The MCH-producing neurons regulate sleep, especially REM sleep, thereby counterbalancing the wake-promoting effect of ORX. In addition to sleep regulation, MCH neurons play an important role in appetite regulation and hippocampus-dependent memories. A study on the rodent model demonstrated that REM sleep-dependent inhibition of MCH neurons impaired hippocampal-dependent memory[16]. Further, Calafate et al. demonstrated that MCH neuronal loss is an early event in AD, downregulates synaptic transmission, modulates firing rates in the hippocampal neurons, and induces sleep defects in the APP^{NL-G-F} mouse model of AD[17]. Despite extensive studies in experimental animals, the knowledge gap for MCH neurons in humans across various neurodegenerative diseases is substantial.

This study provides a comprehensive and quantitative morphological study of orexinergic and MCH neurons and the molecular profile of the LHA in postmortem human brains of subjects across progressive stages of AD and normal controls. We used unbiased stereology and double-labeled immunohistochemistry to quantify the number of ORX and MCH neurons, changes in the proportion of LHA neurons in AD, and the burden of tau pathology to understand the trajectory and pattern of neuronal loss.

Materials and methods:

Participants, selection criteria, and neurological assessment

We carefully selected 33 cases for our study from two cohorts – i) Neurodegenerative Disease Brain Bank (NDBB) at the University of California, San Francisco, and ii) Brazilian BioBank for

bioRxiv preprint doi: https://doi.org/10.1101/2024.03.06.583765; this version posted March 12, 2024. The copyright holder for this preprint (which was not certified by peer review) is the author/funder. All rights reserved. No reuse allowed without permission.

Aging Studies (BBAS) at the University of São Paulo. The NDBB received brains and spinal cords from patients seen at the UCSF Memory and Aging Center. The majority of the NDBB cases consisted of individuals with late-stage dementia. Meanwhile, the BBAS was population-based, with many healthy controls and lower Braak stage cases[18]. The Institutional Review Boards of both participating institutions approved the study. We adhered to standardized protocols for neuropathological assessments and followed the NIA-AA guidelines to assess the staging of AD neuropathologic changes. All subjects received a comprehensive diagnosis based on the neurofibrillary tangle pathology using the Braak stage scale (0 to 6) established by Braak and Braak[19]. We also ensured that all cases had complete neuropathological diagnoses[20] and available measures of functional cognition based on Clinical Dementia Rating (CDR). The demographic details of the cases involved in the study can be found in Table 1.

For the study, we included both male and female participants aged 50-92 years who met specific criteria, including the absence of Lewy body and TDP43, non-AD-related neuropathology (such as argyrophilic granular disease), insignificant cerebrovascular lesions, and an intact hypothalamus. We excluded individuals with neurological disease, neuropsychiatric diagnosis, or non-degenerative structural pathology. To gather comprehensive data, we did a postmortem stereological evaluation of neural numbers for orexin and melanin-concentrating neurotransmitters with CP13 (pTau) inclusions in the LHA. We were mindful of achieving gender balance and maintained a 1:1 female-to-male ratio (18-to-15) for our study.

Tissue processing and immunohistochemistry

bioRxiv preprint doi: https://doi.org/10.1101/2024.03.06.583765; this version posted March 12, 2024. The copyright holder for this preprint (which was not certified by peer review) is the author/funder. All rights reserved. No reuse allowed without permission.

Hypothalamic regions containing LHA^{ORX} and LHA^{MCH} neurons, the area of interest (AOI), were identified using the Allan Human atlas. Formalin-fixed hypothalamic blocks containing the whole AOI were embedded in celloidin and sectioned serially at 30-µm thickness on the coronal or horizontal plane; section orientation does not affect the optical fractionator probe in stereology[21,22]. Every 10^{th} tissue section from the AOI was stained with either i) Orexin A and CP13 antibody combo or ii) MCH and CP13 antibody combo and counter-stained with gallocyanin (pH 1.9-2.1) as described previously[6,7]. In brief, the free-floating serial hypothalamic sections were treated in 0.3% H_20_2 (in methanol) to inactivate endogenous peroxidase and, after that, subjected to 50 mins incubation at 95.7°C in 0.01 M citrate buffer with 0.05% Tween-20 in PBS (pH 6.0) for epitope exposure. To avoid non-specific staining, sections were blocked in blocking buffer (5% milk PBST 0.1% triton X) for 40 mins. Serial sections were double-stained with mouse monoclonal anti-CP13 antibody for phosphor-Ser202 tau (1:1000, a kind gift of Peter Davies, NY, USA) with either rabbit polyclonal anti-Orexin A (1:500, Cat# H-003-30, Phoenix Pharmaceuticals, CA, USA) or rabbit polyclonal anti-MCH serum (1:1000, PBL 234, a kind gift of Joan Vaughan, Salk Institute, CA) overnight at room temperature.

Following overnight primary antibody incubation, the sections were incubated in secondary biotinylated anti-rabbit IgG (1:400, Cat# BA-1100, Vector Labs, CA, USA) and secondary conjugated-HRP anti-mouse IgG (1:400, cat# R-05071-500, Advansta, CA, USA) for 1.5 hours at room temperature. The stained sections were then developed using immPACT DAB Peroxidase (HRP) Substrate Kit (Cat# SK-4150, Vector Labs, CA, USA), Vectastain ABC-AP kit (Cat#AK-5000, Vector Labs, CA, USA), and Vector Red chromogen (Cat# SK-5105, Vector Lab, CA, USA). To estimate the total number of neurons, all sections were counterstained using

bioRxiv preprint doi: https://doi.org/10.1101/2024.03.06.583765; this version posted March 12, 2024. The copyright holder for this preprint (which was not certified by peer review) is the author/funder. All rights reserved. No reuse allowed without permission.

gallocyanin (Cat# A12936, Alfa Aesar, MA, USA) as a nucleic acid stain at a previously optimized pH (pH 1.9 - 2.1).

We performed double immunohistochemistry of MCH and ORX To rule out possible co-expression of these two markers. Supp. Figure S1 depicts representative staining showing the absence of co-expression of these two markers.

Unbiased stereology

The stereological analyses were performed using the StereoInvestigator v.10 software (MBF Bioscience, VT, USA). LHA^{ORX} and LHA^{MCH} neurons of the lateral hypothalamic area were visualized, and live images were captured using a high-resolution camera (MBF, Bioscience, Williston, VT, USA) attached to an Axio Imager.A2 microscope (Carl Zeiss Microscopy, NY, USA). Counting was made for ORX-positive (ORX+ Tau-) or MCH-positive (MCH+ Tau-), tau-positive (ORX- Tau+ or MCH- Tau+), ORX or MCH and tau-positive (ORX+ Tau+ or MCH+ Tau+), and double negative neurons (ORX- Tau- or MCH- Tau-) using the optical fractionator probe[23]. The AOI was delineated at 20x (Plan-APOCHROM 20x/0.8 ∞/0.17, Carl Zeiss Microscopy, NY, USA), and the neuronal counting was performed using a 63x (Plan-APOCHROM 63x/1.4 Oil ∞/0.17, Carl Zeiss Microscopy, NY, USA) objective. The stereological parameters were determined using the "resample–oversample" analysis probes in the StereoInvestigator software[24]. The guard zone was set at 5 µm, and the dissector height at 12.5 µm; for neuronal count settings, refer to Table 2. The coefficient of error (CE) range was calculated following the methods of Gundersen and Schmitz-Hof[25,26] (Table 2).

bioRxiv preprint doi: https://doi.org/10.1101/2024.03.06.583765; this version posted March 12, 2024. The copyright holder for this preprint (which was not certified by peer review) is the author/funder. All rights reserved. No reuse allowed without permission.

Statistical analyses

Mean differences in stereological estimates were assessed between Braak groups for LHA^{ORX} and LHA^{MCH} neurons as population and proportions for each subpopulation (e.g., ORX+ Tau- neurons, ORX+ Tau+ neurons). The proportion of neurons positive for different subpopulations was determined by dividing the number of neurons positive for a given marker by the total neuron population, represented as a percent. The density of neurons was calculated by dividing the neuronal number of specific types by the volume of LHA^{ORX} or LHA^{MCH} neurons. Differences in neuronal numbers and proportion were analyzed using the Wilcoxon signed-rank test, with the alpha level set at 0.05. All analyses were conducted using R-software (version 3.4.4; R Foundation for Statistical Computing, Vienna, Austria).

Results

Stereological estimation of orexinergic neurons in the Lateral hypothalamic area

The optical fractionator method uses a systemic random sampling technique to estimate neuronal numbers in an unbiased manner. The unbiased stereological assessment of the LHA demonstrated a significant decline in total (LHA^{Total}) neuronal number across the progressive stages of AD. The decline in LHA^{Total} neurons started very early in the disease, i.e., from BB 2, where we observed a 47% decline (p=0.0158) over BB 0-1. By the late stage of the disease (BB 5-6), only 24% of neurons (p=0.0043) survived in the LHA compared to the BB 0-1. The profound loss of orexinergic (LHA^{ORX}) neurons across the progressive stages of AD contributed to the global loss of LHA^{Total} neurons. The decline in LHA^{ORX} neurons was progressive, starting from BB 2 (-56%, p=0.0634) and continuing to BB 3-4 (-53%, p=0.0051) and BB 5-6 (-82%, p=0.0043) over BB 0-1 the healthy control (Figure 1).

bioRxiv preprint doi: https://doi.org/10.1101/2024.03.06.583765; this version posted March 12, 2024. The copyright holder for this preprint (which was not certified by peer review) is the author/funder. All rights reserved. No reuse allowed without permission.

In conjunction with a decline in LHA^{ORX} neurons, we observed a significant increase in pTau inclusions in the AOI across progressive stages of AD. In the AOI, we counted pTau inclusions in the LHA^{ORX} and neurons devoid of orexin (LHA^{ORX-}). The proportion of pTau-inclusion in the LHA^{ORX-} neurons significantly increased by 0.58% (p=0.0025) and 1.58% (p=0.0043) in BB 3-4 and BB 5-6 compared to BB 0-1. In contrast, the proportion of pTau inclusion in LHA^{ORX} neurons demonstrated an insignificant change in BB 2 (0.13%, p=0.7086) and BB 3-4 (0.74%, p=0.3434). However, a significant increase in the pTau inclusion in LHA^{ORX} by 5.17% (p=0.0303) was seen in BB 5-6 compared to BB 0-1 (Table 3).

Stereological estimation of melanin-concentrating hormone (MCH) neurons in the lateral hypothalamic area

The LHA plays a critical role in sleep-wake modulation through the wake-promoting orexinergic neurons (LHA^{ORX}) and sleep-promoting MCH neurons (LHA^{MCH}). Following assessing the LHA^{ORX} neurons, we estimated the total number of neurons in the area associated with LHA^{MCH} neurons. Unlike the significant loss of LHA^{ORX} or LHA^{Total} neurons, the LHA^{MCH} neurons demonstrated a more preserved profile. The total number of neurons in LHA with MCH neurons demonstrated an insignificant decline of 25% (p=0.1331). Similarly, the LHA^{MCH} neuronal population also demonstrated a 27% (p=0.1088) decline in BB 6 over BB 0-2 (Figure 2).

Further, we investigated the pTau inclusion pattern in the AOI to understand the vulnerability pattern or resilience of MCH neurons to AD-tau toxicity. We analyzed the proportion of neurons with pTau inclusion in MCH+ (LHA^{MCH+}) and MCH- (LHA^{MCH-}) neurons in the LHA. The

bioRxiv preprint doi: https://doi.org/10.1101/2024.03.06.583765; this version posted March 12, 2024. The copyright holder for this preprint (which was not certified by peer review) is the author/funder. All rights reserved. No reuse allowed without permission.

proportion of pTau inclusion LHA^{MCH+} and LHA^{MCH-} neurons demonstrated a significant increase in the late stage of the disease. Where LHA^{MCH-} neurons demonstrated higher pTau inclusion (7.68%, p=0.0007) than that of LHA^{MCH+} (5.91%, p=0.0006) neurons in BB 6 over BB 0-2 (Table 4).

Discussion

The present study leaps over our previous findings of profound loss of wake-promoting neurons in the subcortical areas in AD[7]. Here, we systemically studied the two neuronal populations of the lateral hypothalamic area (LHA), which play a critical role in sleep-wake modulation in AD. We used stereology for unbiased estimation of neuronal populations of wake-promoting orexinergic and the sleep-promoting melanin concentration hormone neurotransmitter system.

Here, we demonstrated a significant decline (-47%) in the total number of neurons in the LHA (associated with ORX neurons) very early in the disease, i.e., in Braak group 2 over Braak 0-1. This decline in neuronal number continued progressively with the progression of AD. The loss of ORX neurons primary steer this global loss of neurons in the area of interest at the early stage of the disease. We observed a 56% decline in the ORX neuronal population in Braak group 2. However, this change failed to reach the significance levels probably due to fewer cases. The decline demonstrated significance in Braak groups 3-4 and 5-6. A probable confounding factor of missing the significance in Braak group 2 is the fact that there are fewer participants. We also observed a significant increase in pTau inclusions in ORX positive and ORX negative neurons in Braak groups 3-4 and 5-6. Our results indicated that ORX neurons in the LHA are vulnerable to AD-specific tau-toxicity, as tau accumulation was seen early in the disease. In stark contrast, we

bioRxiv preprint doi: https://doi.org/10.1101/2024.03.06.583765; this version posted March 12, 2024. The copyright holder for this preprint (which was not certified by peer review) is the author/funder. All rights reserved. No reuse allowed without permission.

found no such change in the MCH neuronal population even in late Braak stage 5-6. We examined neurons surrounding the MCH neurons in the LHA. We observed a relatively preserved number of MCH-positive neurons, while the proportion of MCH-negative neurons significantly declined. At the same time significant increase in pTau inclusions were observed in the area of interest however the proportion of such neurons were 6 and 8% respectively. Our stereological data demonstrated that ORX neurons were selectively more vulnerable to AD-specific pTau than the neighboring MCH neuronal populations in the LHA. Aging, per se, is considered the primary risk factor for neurodegenerative disorders, including Alzheimer's disease[27]. Using male Fisher 344/Brown Norway F1 hybrid rats, Kessler et al. demonstrated that age-dependent neuronal loss in the LHA was not global. They quantified the immunoreactivity of ORX and MCH neurons in the male rats. They observed a significant decline (~40%) in ORX immunoreactivity to the medial and lateral areas of the fornix. Meanwhile, the decline in MCH immunoreactivity in the LHA was restricted to the area medial to the fornix[28]. A study of normal aging in humans (without any neuropathology) also demonstrated an age-dependent 10% ($p=0.023$) loss of ORX neurons in older adults (48-60 years) over young adults (22-32 years)[29]. A human study with AD patients of Braak stage 5-6 and Braak stage 0-1 demonstrated a significant decline ($p=0.049$) in ORX neurons in the LHA. Further, they showed a significant loss of CSF-ORX levels in AD, and the levels of CSF-ORX correlated negatively with excessive day sleepiness[30]. The loss of ORX neurons in the late stage of human AD patients corroborates with our findings of the present study and previous studies[6,7]; however, the extent of the decline in ORX neurons in AD patients was significantly greater in our studies, which could be associated with our précised unbiased and random system sampling using the stereology while the other study used a conventional counting strategy.

bioRxiv preprint doi: https://doi.org/10.1101/2024.03.06.583765; this version posted March 12, 2024. The copyright holder for this preprint (which was not certified by peer review) is the author/funder. All rights reserved. No reuse allowed without permission.

This study, for the first time, demonstrated that ORX neurons start pTau accumulation very early in the disease and, at the same time, start to degenerate. Targeting the preservation of ORX neurons will be instrumental in treating sleep-wake dysfunction in AD patients, given the role ORX neurons play in maintaining wakefulness and arousal. This could also improve the quality of life for AD patients. In addition to improving sleep-wake homeostasis, therapeutics aimed at preserving ORX systems could also lead to deterring AD progression. Various studies on rodents and in vitro models have demonstrated that ORX administration and/or ORX receptor modulation induce neuroprotection and restore sleep-wake homeostasis by modulation of AKT phosphorylation, ERK pathways, and inflammation[31–36].

MCH plays an important role in maintaining REM sleep[37,38]. Loss or destruction of MCH neurons promotes arousal and wakefulness, with a decrease in non-REM sleep. Hyperactivity of MCH neurons can lead to more REM sleep at the expense of slow wave sleep (SWS)[39,40]. A recent study from our group demonstrated a difference in sleep architecture across AD phenotypes, where REM sleep didn't show any change over controls in amnestic or typical AD patients[41]. Our current finding of preserved MCH neurons in the LHA among AD patients supports the finding of preserved REM sleep in typical AD patients.

In Conclusion, the ORX neurons of the lateral hypothalamic area demonstrated a selective neuronal vulnerability to AD-specific pTau from a very early stage of the disease, while the neighboring MCH neurons were comparatively more resilient, with pTau burden being substantial.

bioRxiv preprint doi: https://doi.org/10.1101/2024.03.06.583765; this version posted March 12, 2024. The copyright holder for this preprint (which was not certified by peer review) is the author/funder. All rights reserved. No reuse allowed without permission.

Therefore, the ORX system can be a potential target to remediate sleep-wake dysfunction and improve the quality of life of AD patients.

Acknowledgment

This work was supported by grants from Tau Consortium/Rainwater Charity Foundation, NIA R01AG060477, NIA R01 AG064314, NIA K24 AG053435 (Grinberg).

Conflict of Interest

The authors do not have any conflict of interest to disclose.

Reference

1. 2023 Alzheimer's disease facts and figures. *Alzheimer's & Dementia*. 2023;19(4):1598-1695. doi:10.1002/alz.13016
2. Sperling RA, Aisen PS, Beckett LA, et al. Toward defining the preclinical stages of Alzheimer's disease: Recommendations from the National Institute on Aging-Alzheimer's Association workgroups on diagnostic guidelines for Alzheimer's disease. *Alzheimer's and Dementia*. 2011;7(3):280-292. doi:10.1016/j.jalz.2011.03.003
3. Musiek ES, Xiong DD, Holtzman DM. Sleep, circadian rhythms, and the pathogenesis of Alzheimer Disease. *Exp Mol Med*. 2015;47(3). doi:10.1038/EMM.2014.121
4. Maestri M, Carnicelli L, Tognoni G, et al. Non-rapid eye movement sleep instability in mild cognitive impairment: A pilot study. *Sleep Med*. 2015;16(9):1139-1145. doi:10.1016/j.sleep.2015.04.027
5. Brzecka A, Leszek J, Ashraf GM, et al. Sleep disorders associated with Alzheimer's disease: A perspective. *Front Neurosci*. 2018;12(MAY). doi:10.3389/fnins.2018.00330
6. Oh JY, Walsh CM, Ranasinghe K, et al. Subcortical Neuronal Correlates of Sleep in Neurodegenerative Diseases. *JAMA Neurol*. 2022;79(5):498-508. doi:10.1001/jamaneurol.2022.0429
7. Oh J, Eser RA, Ehrenberg AJ, et al. Profound degeneration of wake-promoting neurons in Alzheimer's disease. *Alzheimer's and Dementia*. 2019;15(10):1253-1263. doi:10.1016/j.jalz.2019.06.3916
8. Hagan JJ, Leslie RA, Patel S, et al. *Orexin A Activates Locus Coeruleus Cell Firing and Increases Arousal in the Rat*. Vol 96.; 1999. www.pnas.org.
9. Inutsuka A, Yamanaka A. The physiological role of orexin/hypocretin neurons in the regulation of sleep/wakefulness and neuroendocrine functions. *Front Endocrinol (Lausanne)*. 2013;4(MAR). doi:10.3389/fendo.2013.00018
10. Kalló I, Omrani A, Meye FJ, de Jong H, Liposits Z, Adan RAH. Characterization of orexin input to dopamine neurons of the ventral tegmental area projecting to the medial

bioRxiv preprint doi: https://doi.org/10.1101/2024.03.06.583765; this version posted March 12, 2024. The copyright holder for this preprint (which was not certified by peer review) is the author/funder. All rights reserved. No reuse allowed without permission.

prefrontal cortex and shell of nucleus accumbens. *Brain Struct Funct*. 2022;227(3):1083-1098. doi:10.1007/s00429-021-02449-8

11. Calva CB, Fayyaz H, Fadel JR. Increased acetylcholine and glutamate efflux in the prefrontal cortex following intranasal orexin-A (hypocretin-1). *J Neurochem*. 2018;145(3):232-244. doi:10.1111/jnc.14279
12. Aracri P, Banfi D, Pasini ME, Amadeo A, Becchetti A. Hypocretin (Orexin) regulates glutamate input to fast-spiking interneurons in layer v of the Fr2 region of the murine prefrontal cortex. *Cerebral Cortex*. 2015;25(5):1330-1347. doi:10.1093/cercor/bht326
13. Liguori C, Romigi A, Nuccetelli M, et al. Orexinergic system dysregulation, sleep impairment, and cognitive decline in Alzheimer disease. *JAMA Neurol*. 2014;71(12):1498-1505. doi:10.1001/jamaneurol.2014.2510
14. Davies J, Chen J, Pink R, et al. Orexin receptors exert a neuroprotective effect in Alzheimer's disease (AD) via heterodimerization with GPR103. *Sci Rep*. 2015;5. doi:10.1038/srep12584
15. Wang Q, Cao F, Wu Y. Orexinergic System in Neurodegenerative Diseases. *Front Aging Neurosci*. 2021;13. doi:10.3389/fnagi.2021.713201
16. Izawa S, Chowdhury S, Miyazaki T, et al. *REM Sleep-Active MCH Neurons Are Involved in Forgetting Hippocampus-Dependent Memories*. Vol 365.; 2019. https://www.science.org
17. Calafate S, Özturan G, Thrupp N, et al. Early alterations in the MCH system link aberrant neuronal activity and sleep disturbances in a mouse model of Alzheimer's disease. *Nat Neurosci*. 2023;26(6):1021-1031. doi:10.1038/s41593-023-01325-4
18. Grinberg LT, Lucena Ferretti RE, Farfel JM, et al. Brain bank of the Brazilian aging brain study group - A milestone reached and more than 1,600 collected brains. *Cell Tissue Bank*. 2007;8(2):151-162. doi:10.1007/s10561-006-9022-z
19. Braak H, Braak E. Neuropathological stageing of Alzheimer-related changes. *Acta Neuropathol*. 1991;82(4):239-259. doi:10.1007/BF00308809
20. Suemoto CK, Ferretti-Rebustini REL, Rodriguez RD, et al. Neuropathological diagnoses and clinical correlates in older adults in Brazil: A cross-sectional study. *PLoS Med*. 2017;14(3). doi:10.1371/journal.pmed.1002267
21. Heinsen H, Arzberger T, Schmitz C. *Celloidin Mounting (Embedding without Infiltration)-a New, Simple and Reliable Method for Producing Serial Sections of High Thickness through Complete Human Brains and Its Application to Stereological and Immunohistochemical Investigations*. Vol 20.; 2000. www.elsevier.com/locate/jchemneu
22. Theofilas P, Polichiso L, Wang X, et al. A novel approach for integrative studies on neurodegenerative diseases in human brains. *J Neurosci Methods*. 2014;226:171-183. doi:10.1016/j.jneumeth.2014.01.030
23. West MJ, Slomianka L, Gundersen HJG. Unbiased stereological estimation of the total number of neurons in the subdivisions of the rat hippocampus using the optical fractionator. *Anat Rec*. 1991;231(4):482-497. doi:10.1002/ar.1092310411
24. Slomianka L, West MJ. Estimators of the precision of stereological estimates: An example based on the CA1 pyramidal cell layer of rats. *Neuroscience*. 2005;136(3):757-767. doi:10.1016/j.neuroscience.2005.06.086
25. Gundersen HJG, Jensen EBV, Kiêu K, Nielsen J. The efficiency of systematic sampling in stereology - Reconsidered. *J Microsc*. 1999;193(3):199-211. doi:10.1046/j.1365-2818.1999.00457.x

bioRxiv preprint doi: https://doi.org/10.1101/2024.03.06.583765; this version posted March 12, 2024. The copyright holder for this preprint (which was not certified by peer review) is the author/funder. All rights reserved. No reuse allowed without permission.

26. Schmitz C, Hof PR. Design-based stereology in neuroscience. *Neuroscience*. 2005;130(4):813-831. doi:10.1016/j.neuroscience.2004.08.050
27. Hou Y, Dan X, Babbar M, et al. Ageing as a risk factor for neurodegenerative disease. *Nat Rev Neurol*. 2019;15(10):565-581. doi:10.1038/s41582-019-0244-7
28. Kessler BA, Stanley EM, Frederick-Duus D, Fadel J. Age-related loss of orexin/hypocretin neurons. *Neuroscience*. 2011;178:82-88. doi:10.1016/j.neuroscience.2011.01.031
29. Hunt NJ, Rodriguez ML, Waters KA, Machaalani R. Changes in orexin (hypocretin) neuronal expression with normal aging in the human hypothalamus. *Neurobiol Aging*. 2015;36(1):292-300. doi:10.1016/j.neurobiolaging.2014.08.010
30. Fronczek R, van Geest S, Frölich M, et al. Hypocretin (orexin) loss in Alzheimer's disease. *Neurobiol Aging*. 2012;33(8):1642-1650. doi:10.1016/j.neurobiolaging.2011.03.014
31. Sokołowska P, Urbańska A, Biegańska K, et al. Orexins Protect Neuronal Cell Cultures Against Hypoxic Stress: An Involvement of Akt Signaling. *Journal of Molecular Neuroscience*. 2014;52(1):48-55. doi:10.1007/s12031-013-0165-7
32. Zhou M, Tang J, Li S, Li Y, Zhao M. Orexin dual receptor antagonists, zolpidem, zopiclone, eszopiclone, and cognitive research: A comprehensive dose-response meta-analysis. *Front Hum Neurosci*. 2023;16. doi:10.3389/fnhum.2022.1029554
33. Pallais J, Kotz C, Stanojlovic M. Orexin/hypocretinin in multiple sclerosis and experimental autoimmune encephalomyelitis. *Neural Regen Res*. 2020;15(6):1039-1040. doi:10.4103/1673-5374.270310
34. Becquet L, Abad C, Leclercq M, et al. Systemic administration of orexin A ameliorates established experimental autoimmune encephalomyelitis by diminishing neuroinflammation. *J Neuroinflammation*. 2019;16(1). doi:10.1186/s12974-019-1447-y
35. Stanojlovic M, Pallais JP, Kotz CM. Chemogenetic Modulation of Orexin Neurons Reverses Changes in Anxiety and Locomotor Activity in the A53T Mouse Model of Parkinson's Disease. *Front Neurosci*. 2019;13. doi:10.3389/fnins.2019.00702
36. Li S Bin, Nevárez N, Giardino WJ, De Lecea L. Optical probing of orexin/hypocretin receptor antagonists. *Sleep*. 2018;41(10). doi:10.1093/sleep/zsy141
37. Konadhode RR, Pelluru D, Blanco-Centurion C, et al. Optogenetic stimulation of MCH neurons increases sleep. *Journal of Neuroscience*. 2013;33(25):10257-10263. doi:10.1523/JNEUROSCI.1225-13.2013
38. Jego S, Glasgow SD, Herrera CG, et al. Optogenetic identification of a rapid eye movement sleep modulatory circuit in the hypothalamus. *Nat Neurosci*. 2013;16(11):1637-1643. doi:10.1038/nn.3522
39. Vetrivelan R, Kong D, Ferrari LL, et al. Melanin-concentrating hormone neurons specifically promote rapid eye movement sleep in mice. *Neuroscience*. 2016;336:102-113. doi:10.1016/j.neuroscience.2016.08.046
40. Peyron C, Sapin E, Leger L, Luppi PH, Fort P. Role of the melanin-concentrating hormone neuropeptide in sleep regulation. *Peptides (NY)*. 2009;30(11):2052-2059. doi:10.1016/j.peptides.2009.07.022
41. Falgàs N, Walsh CM, Yack L, et al. Alzheimer's disease phenotypes show different sleep architecture. *Alzheimer's and Dementia*. 2023;19(8):3272-3282. doi:10.1002/alz.12963

bioRxiv preprint doi: https://doi.org/10.1101/2024.03.06.583765; this version posted March 12, 2024. The copyright holder for this preprint (which was not certified by peer review) is the author/funder. All rights reserved. No reuse allowed without permission.

Table 1. Demographic characteristics with the distribution of the cases in each THAL stage, Braak and Braak stage, CERAD score, AD diffused score, ABC score, CDR score, and NIA-Reagan score.

Sample Code	Primary Dx	THAL stage	BRAAK stage	Sex	Age of death (year)	PMI (hours)	ABC score	CREAD score	AD diffused score	APOe genotype	CDR score	Brain weight (grams)	NIA Regan score
B #11	AD	1	3	F	75	15.6	A1,B2,C0	C0	Low	3/4	0	1120	Low
B #12	AD	0	3	F	68	13.6	A0,B2,C0	C0	—	—	0	1206	None
B #15	HC	1	0	M	55	18.8	A0,B0,C0	C0	Moderate	—	0	1206	None
B #17	HC	0	1	M	75	16.3	A0,B1,C0	C0	Absent	—	1	1232	Conflict
B #23	HC	0	2	F	63	10.1		—	None	—	—	—	—
B #28	HC	0	1	M	56	39	—	—	—	—	—	—	—
B #29	HC	—	0	F	66	12.9	—	—	—	—	0	1042	—
B #30	AD	2	5	F	65	20.4	A1,B3,C2	C2	—	—	0	1186	—
B #31	HC	—	0	M	63	16	—	—	—	—	0	1426	—
B #33	AD	3	3	F	78	13.9	—	—	—	—	—	—	—
B #34	HC	0	0	M	77	14.5	A0,B0,C0	C0	Absent	—	0	—	—
B #35	HC	—	0	F	64	—	—	—	—	—	—	—	—
U # 01	ADNC	1	2	F	81	30.3	A1,B1,C0	C0	Absent	—	—	1120	Low
U # 02	AD	5	6	M	63	6	A3,B2,C3	C3	Frequent	3/4	—	1000	High
U # 03	AD	5	6	F	56	4.9	A3,B2,C3	C3	Frequent	3/4	—	986	High
U # 04	AD	5	6	M	69	38.3	A3,B3,C3	C3	Frequent	3/4	—	1060	High
U # 05	AD	-7	6	M	61	14.9	A0,B3,C3	C3	Frequent	—	—		High
U # 06	HC	1	2	M	76	8.2	A1,B1,C1	C1	—	—	—	1324	Low
U # 07	AD	2	4	F	87	9.5	A1,B2,C3	C3	Low	3/3	—	1119	Not applicable
U # 08	AD	5	6	M	60	5.2	A3,B3,C3	C3	Moderate	3/3	—	1140	High
U # 09	AD	5	6	M	59	9	A3,B3,C3	C3	Frequent	3/3	3	1090	High
U # 11	AD	3	5	M	81	9.9	A2,B3,C3	C3	Frequent	3/3	0.5	1264	High
U # 12	AD	5	4	M	91	11.16	A3,B2,C3	C1	Low	3/3	0.5	1036	Intermediate
U # 14	HC	0	2	F	92	7.9	A0,B1,C0	C0	Absent	—	—		Not met
U # 15	AD	5	6	F	62	8.6	A3,B3,C3	C3	Frequent	—	—		High
U # 16	HC	2	1	F	82	9.6	A1,B1,C0	C0	Frequent	3/4	—	1108	Not met
U # 17	AD	5	6	F	67	6.25	A3,B3,C3	C3	Frequent	2/4	—		High
U # 19	AD	2	4	F	92	13	A1,B3,C2	C2	Frequent	3/4	0	1102	Intermediate
U # 20	AD	5	6	F	64	20.8	A3,B3,C3	C3	Frequent	3/3	3	1061	High
U # 21	AD	2	4	M	91	5.6	A1,B2,C1	C1	Frequent	3/3	0	1109	Non-conforming
U # 23	HC	2	2	F	84	7.7	A1,B1,C1	C1	Frequent	3/4	—	1181	Low
U # 25	HC	2	2	M	72	17.3	A2,B1,C0	C0	Moderate	—	—	1282	Non-conforming
U # 28	AD	2	5	F	74	9.8	A3,B3,C3	C3	Frequent	3/3	—	1215	High

bioRxiv preprint doi: https://doi.org/10.1101/2024.03.06.583765; this version posted March 12, 2024. The copyright holder for this preprint (which was not certified by peer review) is the author/funder. All rights reserved. No reuse allowed without permission.

Table 2. Details of stereology parameters used to count orexinergic and melanin-concentrating hormone-producing neurons in the lateral hypothalamic area

	LHA^{ORX}	**LHA^{MCH}**
Optical fractionator (µm2)	120 µm x 120 µm	120 µm x 120 µm
x, y step up (µm2)	210 µm x 210 µm	210 µm x 210 µm
Guard zone	2 µm, 2 µm	2 µm, 5 µm
Dissector height	12 µm	15 µm
Section cut thickness (µm)	30 µm	31 µm
Section interval	10	10
Coefficient of error (CE)	<0.1	<0.1

bioRxiv preprint doi: https://doi.org/10.1101/2024.03.06.583765; this version posted March 12, 2024. The copyright holder for this preprint (which was not certified by peer review) is the author/funder. All rights reserved. No reuse allowed without permission.

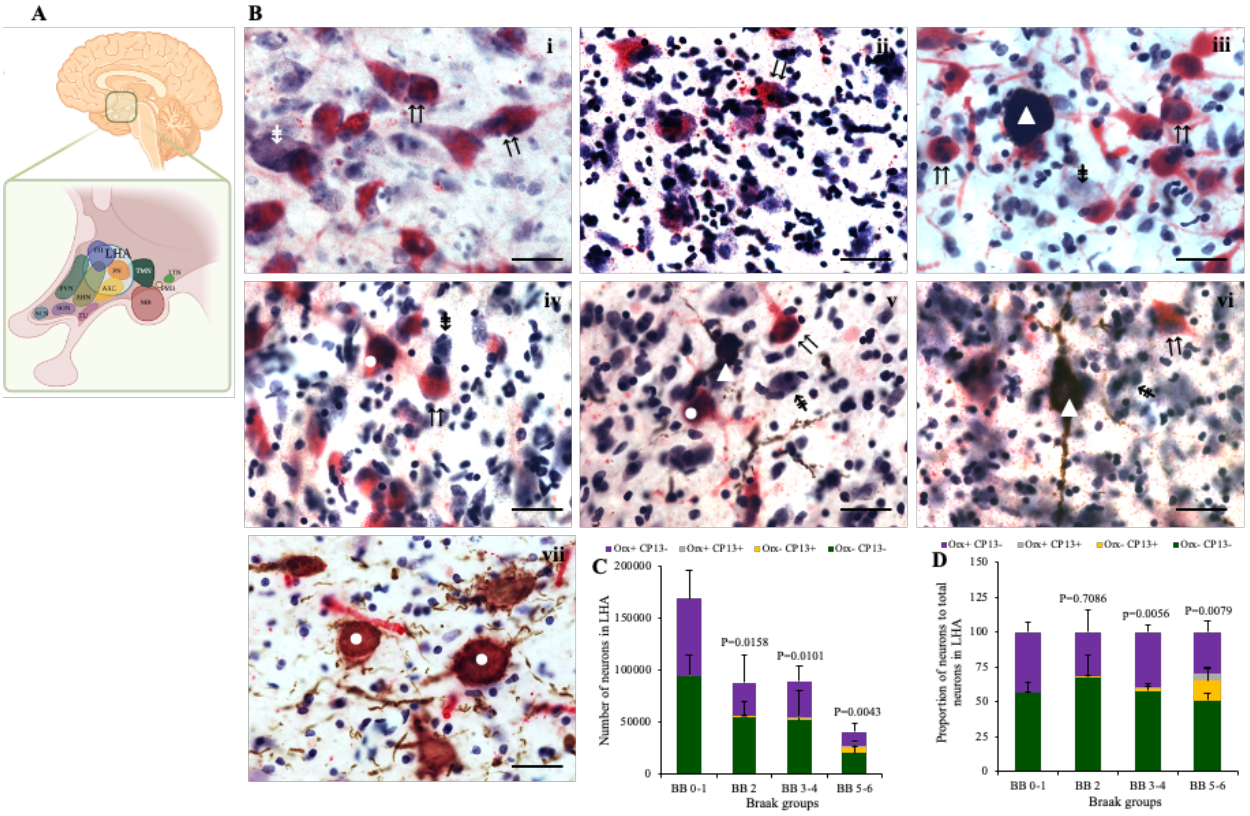

Figure 1. Panel A depicts the location of the LHA in the human brain, while panel B representative microphotographs of Braak 0 (i), Braak 1 (ii), Braak 2 (iii), Braak 3 (iv), Braak 4 (v), Braak 5 (vi) and Braak group 6 (vii) with ORX- CP13- (↡), ORX- CP13+ (▲), ORX+ CP13 + (●), and ORX+ CP13- (⇈) neurons in the LHA with at 63x (scale 20µm). Bar graphs represent mean ±SD values of the number of neurons in LHA (C) and the percent of total neurons in the LHA (D). P values were determined using the Wilcoxon rank-sum test, comparing the different stereological estimates between Braak stage groups. P-values denote the significance level in the total number of neurons over the Braak group 0-1 (C) and the significance level in the proportion of Orx+ CP13- over the Braak group 0-1 (D). Abbreviations: **CP13**, Tau phos Ser202 (pTau inclusions marker); **ORX**, orexin; **SD**, standard deviation; **LHA**, Lateral hypothalamic area.

bioRxiv preprint doi: https://doi.org/10.1101/2024.03.06.583765; this version posted March 12, 2024. The copyright holder for this preprint (which was not certified by peer review) is the author/funder. All rights reserved. No reuse allowed without permission.

Table 3. Mean ± standard deviation of stereological estimates of cell types in the LHA^{ORX} stratified by Braak groups

Number of neurons in LHA^{ORX}					
Braak group	Orx- CP13-	Orx- CP13+	Orx+ CP13+	Orx+ CP13-	Total
BB 0-1 (n=6)	93825.40 ± 20750.13	227.60 ± 158.68	86.20 ± 80.07	74307.80 ± 28031.01	168447 ± 44843.26
BB 2 (n=4)	54909.58 ± 14496.37 *	586.56 ± 651.93	147.81 ± 194.11	32534.80 ± 26109.11 (p=0.06)	88178.75 ± 40577.61 *
BB 3-4 (n=7)	52052.28 ± 28460.61 *	1689.88 ± 1843.37 *	704.31 ± 561.56 **	34767.71 ± 15125.66 **	89214.19 ± 43748.81 *
BB 5-6 (n=6)	20356.29 ± 9900.74 **, $, #	5096.03 ± 2755.66 **	2235.57 ± 2224.3 **,$,$$,#	12639.40 ± 7306.21 **, #	40327.29 ± 18775.05 #
Proportion of neurons to total neurons in LHA^{ORX}					
Braak group	Orx- CP13-	Orx- CP13+	Orx+ CP13+	Orx+ CP13-	
BB 0-1 (n=6)	56.43 ± 7.51	0.15 ± 0.12	0.055 ± 0.05	43.36 ± 7.47	
BB 2 (n=4)	67.63 ± 15.72	0.58 ± 0.47	0.13 ± 0.15	31.67 ± 15.4	
BB 3-4 (n=7)	57.83 ± 4.83	1.78 ± 1.59 **, $	0.74 ± 0.49 **, $	39.65 ± 4.98	
BB 5-6 (n=6)	50.81 ± 5.49	14.15 ± 10.21 **, $$, ##	5.17 ± 3.83 **, $$$, ##	29.87 ± 8.51 **, ##	

P-values were obtained from a Wilcoxon rank-sum test comparing the serological counts of LHA^{ORX} neurons between different Braak stage groups where *p<0.05, **p<0.01, ***p<0.001 (over BB 0-1); $p<0.05, $$p<0.01, $$$p<0.001 (over BB 2); #p<0.05, ##p<0.01, ###p<0.001 (over BB 5-6). Abbreviations: **CP13**, Tau Phos Ser 202; **LHA**, lateral hypothalamic area; **ORX**, orexin; SD, standard deviation.

bioRxiv preprint doi: https://doi.org/10.1101/2024.03.06.583765; this version posted March 12, 2024. The copyright holder for this preprint (which was not certified by peer review) is the author/funder. All rights reserved. No reuse allowed without permission.

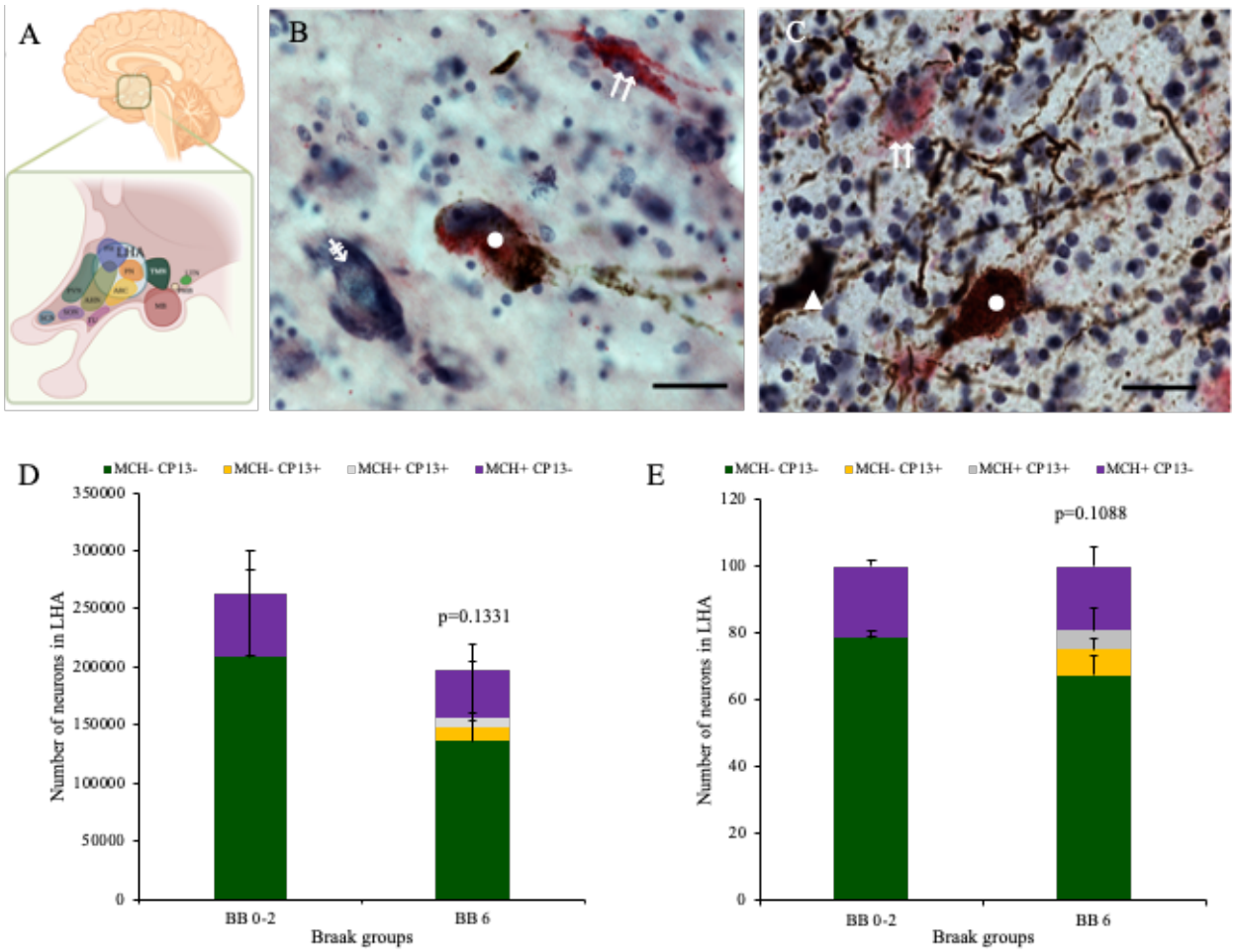

Figure 2. A depicts the location of the LHA in the human brain, representative microphotographs of Braak group 0-2 (B) and Braak group 6 (C) with MCH- CP13- (↡), MCH- CP13+ (▲), MCH+ CP13+ (●), and MCH+ CP13- (↑↑) neurons in the LHA at 63x (scale 20µm). Bar graphs represent mean ±SD values of the number of neurons in LHA (C) and the percent of total neurons in the LHA (D). P values were determined using the Wilcoxon rank-sum test, comparing the different stereological estimates between Braak stage groups. P-values denote the significance level in the total number of neurons over the Braak group 0-2 (C) and the significance level in the proportion of MCH+ CP13- over the Braak group 0-2 (F). Abbreviations: **CP13**, Tau phos Ser202 (pTau inclusions marker); **MCH**, melanin-concentrating hormone; **SD**, standard deviation; **LHA**, Lateral hypothalamic area.

bioRxiv preprint doi: https://doi.org/10.1101/2024.03.06.583765; this version posted March 12, 2024. The copyright holder for this preprint (which was not certified by peer review) is the author/funder. All rights reserved. No reuse allowed without permission.

Table 4. Mean ± standard deviation of stereological estimates of cell types in the LHA stratified by Braak groups

Number of neurons in LHA^{MCH}					
Braak group	MCH- CP13-	MCH- CP13+	MCH+ CP13+	MCH+ CP13-	Total
BB 0-2 (n=7)	226288.79 ± 86063.67	409.43 ± 484.4	14.35 ± 22.26	59012.55 ± 18712.41	263845.09 ± 111330.28
BB 6 (n=10)	135762.71 ± 68829.73	12835.30 ± 4414.82 ***	8245.88 ± 3717.97 ***	39822.68 ± 22202.39	196666.58 ± 94207.94
Proportion of neurons to total neurons in LHA^{MCH}					
Braak group	MCH- CP13-	MCH- CP13+	MCH+ CP13+	MCH+ CP13-	
BB 0-2 (n=7)	78.64 ± 2.19	0.15 ± 0.18	0.004 ± 0.006	21.21 ± 2.11	
BB 6 (n=10)	67.30 ± 5.6 ***	7.68 ± 3.14 ***	5.91 ± 6.6 ***	19.12 ± 5.92	

P-values were obtained from a Wilcoxon rank-sum test comparing the serological counts of LHA^{MCH} neurons between different Braak stage groups where *p<0.05, **p<0.01, ***p<0.001 (over BB 0-1); $p<0.05, $$p<0.01, $$$p<0.001 (over BB 2); #p<0.05, ##p<0.01, ###p<0.001 (over BB 5-6). Abbreviations: **CP13**, Tau Phos Ser 202; **LHA**, lateral hypothalamic area; **MCH**, melanin-concentrating hormone; SD, standard deviation.